

# First light of the 6.5-m MMT adaptive optics system

F. Wildi<sup>1,3</sup>, G. Brusa<sup>1</sup>, M. Lloyd-Hart<sup>1</sup>, L. Close<sup>1</sup>, A. Riccardi<sup>2</sup>

1 – Steward Observatory, Tucson, AZ, U.S.A.

2 – Osservatorio Astrofisico di Arcetri, Firenze, Italy

3 – Now at the Swiss University of Applied Science, Yverdon, Switzerland

## 1. Abstract

The adaptive optics system of the 6.5m MMT with its deformable secondary has seen first light on the sky in November 2002. Since then, it has logged over 30 nights at the telescope and has been used with several scientific cameras and a dedicated IR infrared camera. Results so far are extremely encouraging with Strehls of up to 20% in H-band and 98% in M limited in part by the control algorithm that is being improved. Reliability of the deformable secondary mirror (DM) has been remarkable with only one occurrence of a malfunction that required removing the secondary from its hub.

In this paper, we review the milestones achieved and the performances obtained in the first year of operation. We will also address the operational constraints associated with the deformable secondary and the steps taken to relax these constraints. We show that despite its apparent complexity, an adaptive secondary AO system can be operated with modest effort from the telescope and AO staff

Keywords: Adaptive optics, IR astronomy, high resolution, deformable mirror

## 2. System description

### 2.1. General

Please refer to the numerous previous communications for a detailed presentation of the MMT AO system [see for example 6, 9 and 11]. We will just point out that this adaptive optics uses the secondary mirror of the telescope as wavefront corrector. This layout makes it particularly suitable for thermal infrared astronomy when the number of warm surfaces needs to be minimized while throughput is maximized. It also makes it very attractive for multi-conjugate AO since the secondary is roughly conjugated to the strong ground layer [5]. The price to pay is that the AO system is delocalized on the telescope with the wavefront sensing package separated from the DM. This presents a particular challenge on a telescope like the MMT where up to 3 different secondaries can be used, requiring handling the DM and the removal of all AO-related optics between each mission.

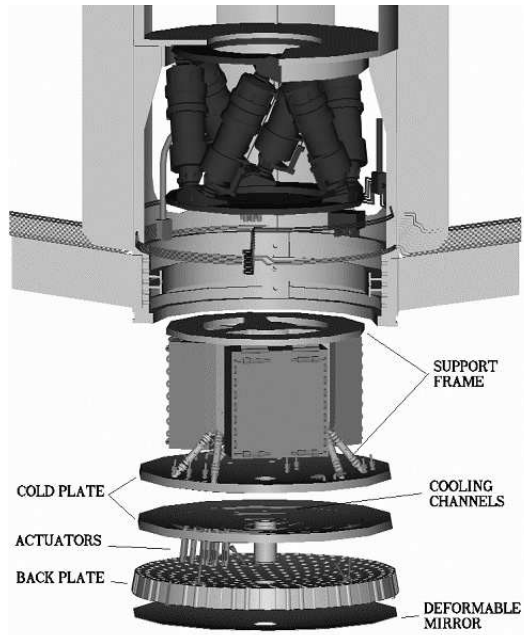
Technology for building large, fast deformable mirrors with comparatively low actuators density has been one of the major undertakings of this project [see 7 and 10.]. The 640mm diameter  $f/15$  deformable secondary mirror has been built and characterized in the past couple of years and has performed very satisfactorily in the laboratory [see also 6]

### 2.2. Deformable mirror breakdown

As a remainder, we review here the main elements of the deformable mirror. In this article, we define the DM as the functional ensemble implementing the function of a reflective surface controlled in position by 336 actuators.

It is made of a *support frame*, 3 *boxes of electronics* hosting the 168 digital signal processors that implement the position control of the deformable face sheet, a *cold plate* in which the 336 actuators are clamped, a *glass reference body* and a deformable glass face sheet called “*shell*” in short that has the optical surface of the secondary mirror.

The cold plate holds the actuators and removes their heat. A water circuit running through the cold plate and the boxes of electronics removes the heat generated by the coil actuators and their drive circuit. The reference body provides a stiff reference surface against which the 336 sensors associated with the 336 actuators measure the local position of the shell



### 2.3. Deployment

The installation of the AO secondary is the most complex and risky part of the AO system deployment at the telescope. It involves removing the traditional solid secondary used for seeing-limited observations and installing the DM including its logistics like power, signal, telemetry and cooling.

The IR-optimized design, using the secondary as the telescope stop does generate constraints on the available space for installation. The secondary hub is designed to be in the shadow of the secondary and therefore is substantially smaller than the secondary itself, creating though clearance constraints. In addition, since the secondary is the stop, all its surface is used and there is no mechanical protection around its edge, creating a safety hazard.

The installation of this unit is complex and potentially risky but over the first 4 runs, we have developed procedures and tools to shorten this operation to around 2 hours and make it safer for the hardware.

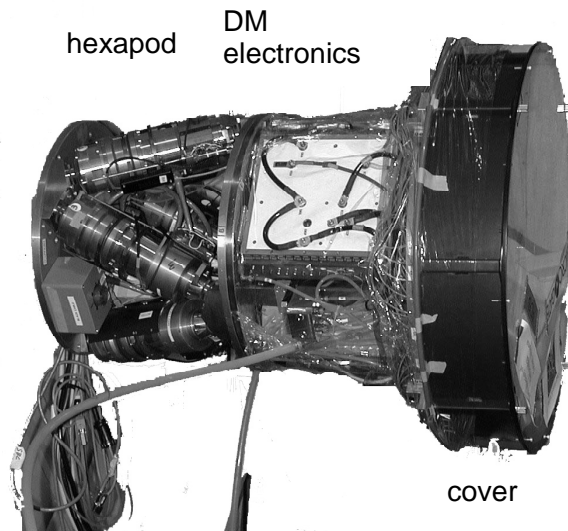


**Figure 2.3-1 Deformable secondary attached to the hexapod. A cover protects the face sheet and the rather extensive cable wrap can be seen hanging below. This complete ensemble is installed into the telescope hub. On this picture, the DM is in the installation position, which is with telescope horizon pointing.**

## 2.4. Evolution

After the technical difficulties encountered during the first mission at the MMT [see 6], a number of modifications were implemented on the deformable mirror. The most important two were

- To implement an external liquid cooling circuit: The original design embedded a cold plate in which the coolant was circulated. Since the cold plate started leaking, it was decided to renounce to cooling the cold plate directly and instead, to clamp a liquid-cooled heat-sink on the side of the cold plate and use the later solely to conduct the heat from the actuators to the heat-sink.
- To increase the cleanliness in and around the mirror in reaction to a number of occurrences when the gap between the face-sheet and the back plate was contaminated by dust. The inside of the DM was thoroughly cleaned and a protective shroud of clean room-grade fabric was tailored around the complete secondary assembly, from the glass back-plate to the rear flange of the support frame

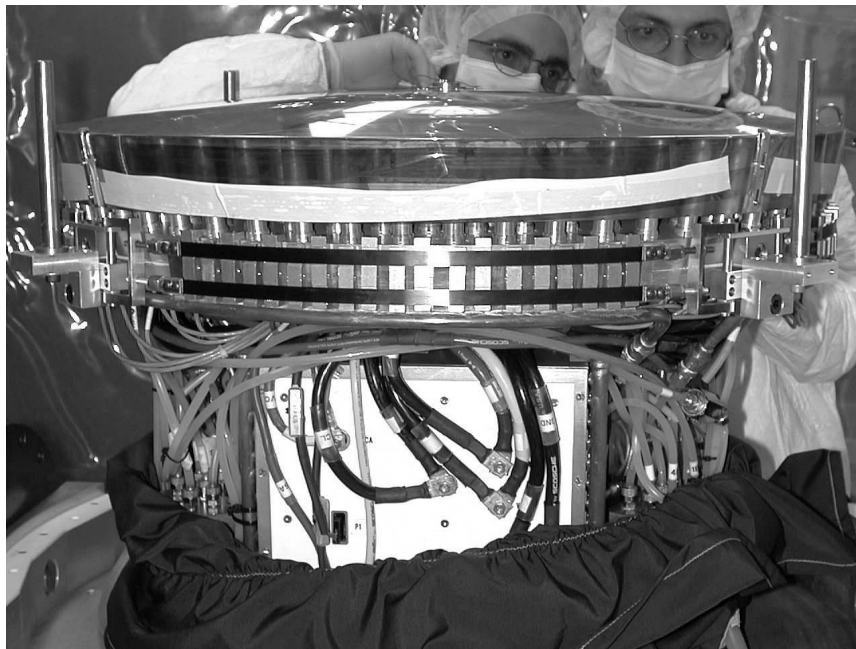


**Figure 2.4-1.** The DM is now equipped with an external liquid cooling circuit that can be seen clamped against the cooling body by the black bands (top half). The fabric shroud can be seen at the bottom, retracted in the clean room for accessibility.

## 3. Preliminary performance evaluation

At this point (summer 2003), the MMT-AO system has performed 3 missions of 2 weeks each. While the 1<sup>st</sup> one was entirely dedicated to engineering, the two following ones included a few night of science observing time that have been spent mostly with the MIRAC M-band camera. We describe below the performance obtained so far:

### 3.1. Set-up

Most of the system characterization was performed with an off-the-shelf TE-cooled camera . This is an INDIGO Merlin fitted with a InGaAs 320x256 array filtered to work in H-band (1.65  $\mu\text{m}$ ). Provided the light level is sufficient, this camera has a level of performance adequate for system engineering and offers functions rarely available on science instruments like the possibility to visualize and acquire frames in real time and take short exposure (down to 1 $\mu\text{s}$ ). At the Cassegrain focus of the telescope, a simple doublet relays the direct f/15 focus of the telescope to the camera.

The science camera used in so far is BLINC/MIRAC [see 12 and 14], a M-band and L-band optimized imager and nulling interferometer. Thanks to the IR detector technology that allows non-destructive read-outs, this instrument has also been convenient for the engineering team, enabling real-time diagnostic of the focal plane images.

### 3.2. System performance

#### 3.2.1. Strehl ratio in H-band

The Strehl ratio achievable so far is  $\cong 20\%$  in H-band, which converts to about 45% in K-band. This result is achieved with a controller implementing a pure integrator and correcting 52 mirror modes at a sampling frequency of 550 Hz. In these conditions, a FWHM of 0.065" is obtained (the diffraction limit of the telescope is 0.060")

It is important to note that the PSF is free from the "waffle" diffraction patterns typically found in the traditional stacked PZT deformable mirrors. The image on the right exemplifies the image quality achieved today. The modest number of modes used is due to the fact that we have set conservative limits on the amount of force we allow the actuators to put in the face sheet. As software is validated and experience is gained, these limits will be relaxed.

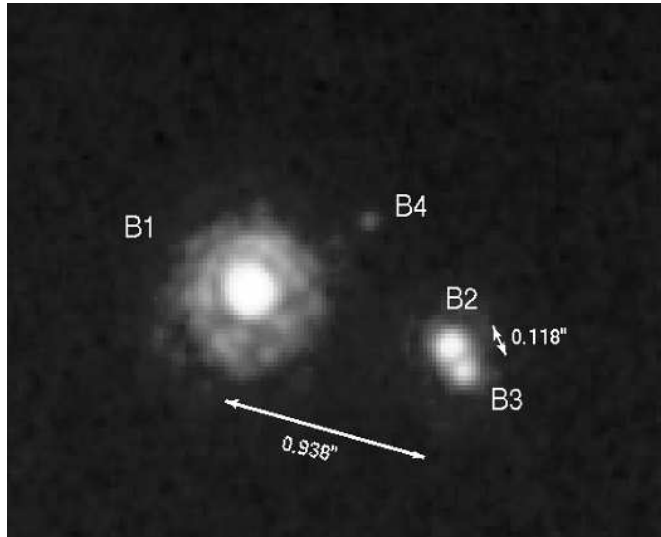


**Figure 3.2-1 Typical image obtained in good seeing conditions. Strehl is 15%. (Detail of the  $\theta^1$  Ori B group as imaged at 0.077" resolution in H band. Logarithmic color scale [see 2])**

#### 3.2.2. Guide star magnitude

The guide star limit magnitude is in the 12-13 mag. with the system running at 200Hz and 52 modes. The parameter space has not yet been fully explored towards the faint objects and we expect that in good seeing conditions, with moderate wind, guide stars of up to magnitude 16 will be reachable (with a smaller number of modes and/or slower sampling speed).

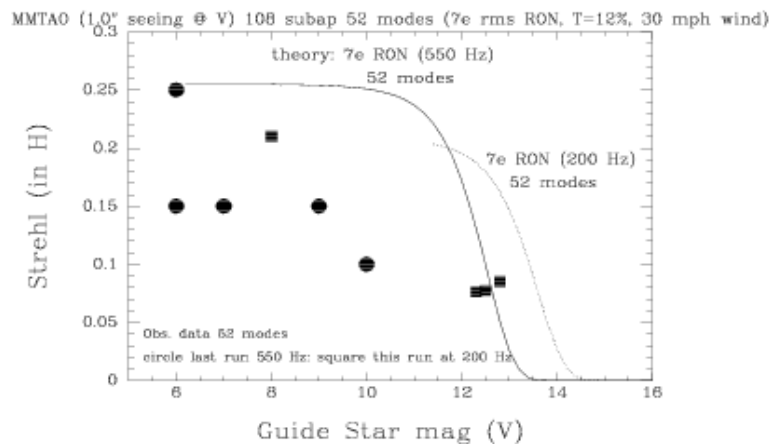


**Figure 3.2-2. Strehl versus GS magnitude graph measured (points) on the sky and the analytical prediction (line). The Strehl is somewhat lower than expected but the limit magnitude corresponds to the expectation at 200Hz .**

### 3.2.3. Performance in M-band

Besides exhibiting a Strehl ratio of 98% at 9.8 $\mu\text{m}$  -which is consistent with the 20% measured in H-band- the M-band PSF is extremely reproducible (to within the measurement error). This feature has already been taken advantage off in one scientific publication [see 1]

In a world première, nulling interferometry has also been performed during closed loop AO, using the BLINC-MIRAC instrument. The null depth achieved was 2%, compared to 5% in seeing-limited operation, an improvement factor of 2.5. Moreover, nulling in seeing-limited conditions is obtained by frame selection of interferograms modulated by the turbulence-induced phase variations of the wavefront. Typically only one in 500 frames is a good null in this operating mode. In the closed-loop AO mode, the null obtained is stable and all frames are usable. This represents a time efficiency increase of almost 3 orders of magnitude!

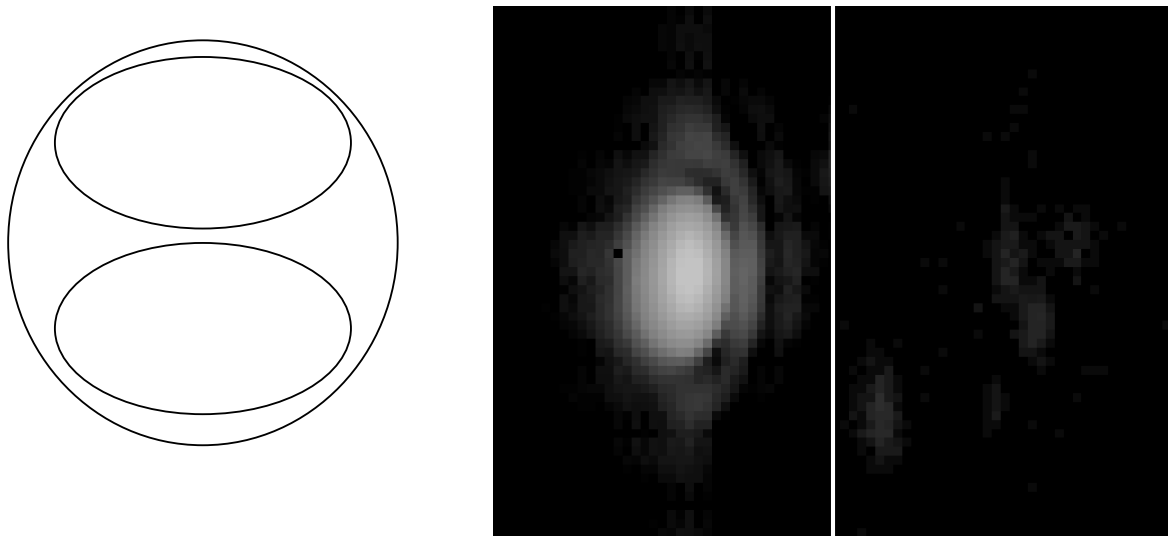


**Figure 3.2-3** This image presents the M-band constructive (center) and destructive (right) interference obtained with the BLINC-MIRAC instrument. The null obtained is only 2% of the constructive image. The PSF is oval because BLINC cuts the telescope pupil in two adjacent pupils and combined them (left).

### 3.3. Present limitations

At the present time, the AO system cannot be considered optimized. We do not take advantage of all the capabilities of the system and certain parameters need to be tuned. Below is a non-exhaustive list of the aspects that limit the performance of the AO

#### 3.3.1. Vibrations

Wavefront residuals measured on the WFS show that the telescope or the AO system vibrates at a frequency around 20Hz and its harmonic at around 40 Hz. The WFS data exhibits a tip motion of  $\cong 20$  milliarcsec rms over the entire frequency spectrum.

Assuming this tip motion is produced by the rocking of the hub around its CoG, this should produce linear acceleration at the external radius of the telescope hub of:

$$a_{lin} = \frac{1}{2} AC \omega^2 \cos(\omega t) \cdot r_{hub}$$

Where  $A$  is the angular amplitude on the sky (in [rad]),  $C$  the compression factor between the primary and the secondary,  $\omega$  the pulsation and  $r_{\text{hub}}$  the radius of the hub. The  $\frac{1}{2}$  factor takes into account the fact that the secondary influences the wavefront in double pass. The numerical value of this expression is  $2.3\text{e-}3$  [ $\text{m/s}^2$ ] or  $2.3\text{e-}4$  [g]

During the most recent run of the AO system, 3-axis accelerometers were installed on the telescope to try to locate the source of the vibrations observed. One was on the secondary hub, one on one of the secondary spider vanes and the last one on the azimuthal yoke of the telescope.

The sensor located on the hub shows a rich spectrum on the z axis precisely in the 20Hz area where the vibrations are observed by the WFS. See figure below. In a typical case, the total amplitude in the 19-20 Hz range is  $1.4\text{e-}3$   $\text{m/s}^2$ . This is in a 1<sup>st</sup> approach consistent with the acceleration derived from the WFS residuals, since they show  $2.3\text{e-}3$   $\text{m/s}^2$  over the entire range. Accelerations measured in the x and y directions are nearly as large as the one in z and therefore excludes that the whole top end of the telescope jitters sideways. However, having just one 3-axis sensor on the hub does not allow to fully describe its motion and therefore, we cannot draw definitive conclusions yet.

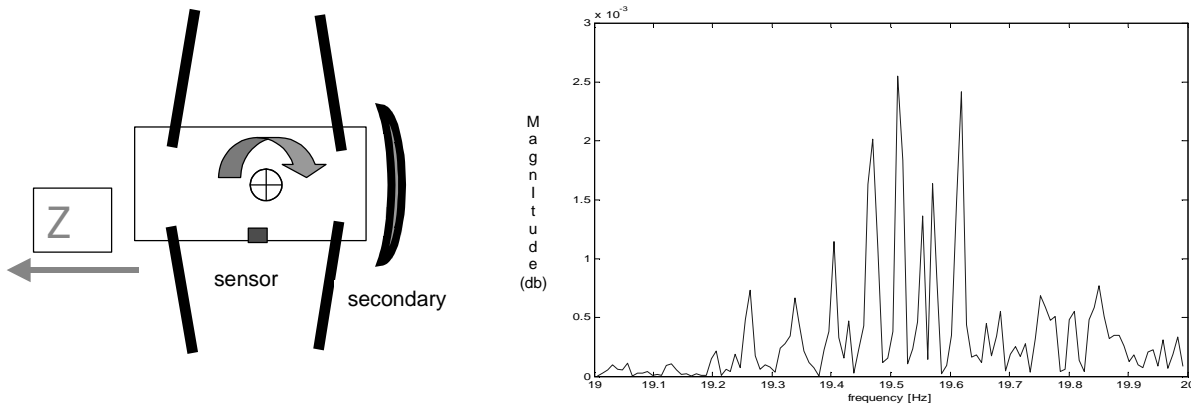


**Figure 3.3-1. The telescope secondary mirror hub is probably rocking around its CoG as suggested on the left. The measured vibration spectrum exhibits a set of lines in the 19-20Hz consistent to what we measure with the WFS.**

Clearly more measurements are required to identify which are the modes in which the secondary hub vibrates and how this vibration is possibly induced by other telescope elements. This needs to be an iterative approach in which the measurements feed the FEA models and the FEA models define the additional measurements required. The next step that we propose is to instrument the secondary hub with 3 accelerometers so as to fully determine its rigid-body motion.

### 3.3.2. Controller

Up to now, the controller implements a pure integrator only, with gains settable individually for each mode. However, no effort has been made to adjust the individual gains to the night conditions, nor to implement more a sophisticated algorithm. The controller architecture provides for a 5-tap FIR filter the input of which is the WFS signal (no feedback of the DM position). As soon as the workload permits, we intend to implement a 5-tap approximation of a Smith predictor [see 13] on the system. This should allow us to gain about 40 Hz of closed-loop bandwidth as one can see on the figure below. The Smith predictor is not sufficient, however, to compensate for the vibration as it does only marginally affect the error rejection function (0.0 dB moves from 22.4Hz to 24.2Hz). This justifies investing resources in the elimination of the source of the vibration.

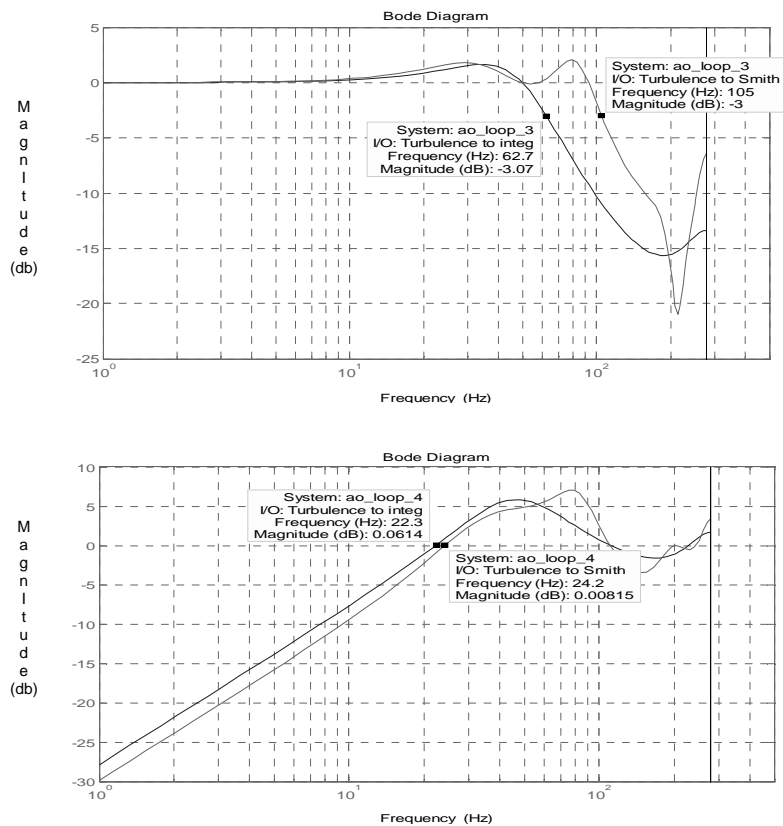


**Figure 3.3-2. The introduction of a Smith predictor is expected to enhance substantially the closed-loop bandwidth of the AO loop (top graph). However, the rejection function, which is the criterion for vibration rejection, will hardly improve (bottom graph).**

### 3.3.3. Non-common path

The influence of non-common path aberrations has not been quantified yet. During closed-loop AO, the operator removed obvious aberrations observed in the science image planes in semi-real time by biasing the slopes measured by the WFS. However, the precision of this correction is limited by the number of modes that can be seen by a human eye and by the threshold level at which they can be seen. We are only now starting to reduce the real-time science plane images taken so far and are hoping that in the near future, we can make tools available to extract the amplitude of low order aberrations at the focal plane on-the-fly and feed it back into the Wavefront Computer for immediate correction.

## 3.4. Extensions

Apart from improving the performance achieved so far, the group is also working to extend the capability of the system. In particular, the work is now focusing on 2 exciting features:

- A procedure to permit the measurement of the interaction matrix on the sky has been developed and is being implemented. Only the weather at the end of last run prevented test data to be acquired to validate the technique. This is to our knowledge the only AO system that features this capability, which is desirable to optimize the real-time reconstructor. Note that our system requires this capability because, unlike in traditional AO system, an artificial star cannot be shone easily into the adaptive secondary system to calibrate the interaction matrix. [see 4]

- Chopping will be introduced at the secondary mirror level. The AO system will perform both the atmospheric compensation and a 10 Hz chopping motion with its single deformable mirror, a perspective that is extremely promising for thermal infrared astronomy. The optical loop will be closed on one of the 2 chop phases while it will stay open during the other phase. The chopping is phased by the science camera so that any chopping-capable instrument can be interfaced to the AO.

Work is also proceeding in the area of science instrument integration with the goal of controlling the AO and the telescope directly from the instrument user interface.

## 4. Operational considerations

### 4.1. *Lessons learned*

The MMT-AO team at the Center for Astronomical Adaptive Optics has been through a steep learning curve in 2002-2003. The system has had major upgrades at each of the 3 runs following the 1<sup>st</sup> attempt and is entering a period of consolidation. It has shown a great flexibility.

Below is a list of the major lessons that can be drawn from the first year of operation at the telescope

- It is possible to a mount, operate and dismount the Adaptive Secondary without breaking it. Four missions have demonstrated however, that strict procedures and efficient tooling play an essential role in operating the system safely.
- Installation and alignment of the complete system is now well understood and cost slightly over a day and a night of telescope time. This figure is expected to drop somewhat, as the crew gets more proficient at analyzing alignment errors.
- The DM is able to operate for extended periods of time without gap contamination. Internal cleanliness seem to play a more important role than air-borne particles in keeping the DM operational over extended periods of time. Keeping the inside of the DM assembly clean during assembly and maintenance and enclosing it in a protective suit seems to be critical.
- The DM is operable even with a significant number of failed actuators. Unlike traditional piezo-stack deformable mirrors, the technology used in the deformable secondary allows failed actuators. Excellent closed optical loop results were obtained in the lab with 4 actuators off, during the first MMT mission, we lost another 9 (because of leaks) with minimal impact on the figure and no impact on the response. It is worth noting that no actuator has failed during the last 3 operational runs.
- Thanks to its stable calibration, the DM can be operated as a traditional solid secondary for seeing-limited observations
- In such a complicated and compact system, there is little space for errors and we feel lucky that we were able to recover from the failure of the cooling system without too much of a penalty

## 5. Conclusion

The MMT-AO system has seen first light at the end of 2002 and has quickly shown good performance leading to several astronomy publications. We are particularly pleased with the obvious lack of “waffle modes” in the secondary and the effect this has on the smoothness of the PSF.

The system has shown to be rather easier to operate than anticipated. In particular, the installation and alignment of the system on the telescope is now well understood and documented. Steps are taken to allow the system to transition from its present experimental state to being a facility instrument largely taken in charge by the MMT operation crew.

Characteristics of the system limiting the performance have been identified and manpower is allocated to correct the system. Pushing the performance limits requires work in the mechanical/control area as well as work in image processing and real-time software development.

The academic year 2003-2004 will be a transition year for the MMT-AO where engineering will give way to science and the development crew will hand over the system to the operation crew.

## 6.Acknowledgments

This work is supported by a grant from the Air Force Office of Scientific Research. Grand AFOSR#F49620-01-1-0383. The achievements presented here were only made possible by the dedication of an entire team of scientists, engineers and technicians, which we congratulate for their success, efficient support and their dedication to the program.

## 7.References

1. "Mid-infrared images of post AGB star AC Herculis with the MMT Adaptive optics system", L. Close, B. Biller, W. Hoffmann, P. Hinz, J. Biegging, F. Wildi, M. Lloyd-Hart, G. Brusa, D. Fisher, D. Miller, R. Angel. submitted to ApJ letters
2. "High resolution images of orbital motion the trapezium cluster: first scientific results from the MMT deformable secondary mirror adaptive optics system". L. Close, F. Wildi, M Lloyd-Hart, G. Brusa, D. Fisher, D. Miller A. Riccardi, P. Salinari, D. McCarthy, R. Angel, R. Allen, H. Martin, R. Sosa, M. Montoya, M. Rademacher, M. Rascon, D. Curley, N. Siegler, W. Duschl. Submitted to ApJ
3. M.. Lloyd-Hart , F. Wildi, G. Brusa, "Lessons learned from the first adaptive secondary mirror", SPIE international symposium on Optical Science and technology, 4-5 August 2003, San Diego CA, USA (5169-10)
4. G. Brusa, A. Riccardi, F. Wildi, M. Lloyd-Hart, H. Martin, R. Allen, D. Fisher, D. Miller, P. Salinari, R. Biasi, D. Gallieni, and F. Zocchi. "MMT adaptive secondary: First AO closed-loop results", SPIE international symposium on Optical Science and technology, 4-5 August 2003, San Diego CA, USA (5169-04)
5. D. McKenna, R. Avila, J. Hill, S. Hippler, P. Salinari, P. Stanton, R. Weiss, "LBT facility SCIDAR: first results", SPIE conference on Adaptive Optical System Technologies II, 4839, Kona 2002, to be published.
6. F. Wildi, G. Brusa, D. Miller, D. Fisher, R. Allen, M.. Lloyd-Hart, A. Riccardi, H. Martin. "Towards 1<sup>st</sup> light of the 6.5m MMT adaptive optics system with deformable secondary mirror", SPIE Conference on Astronomical Telescopes and Instrumentation, 22-28 August 2002, Waikoloa, Hawaii, USA. (4839-19)
7. A. Riccardi, G. Brusa, C. Del Vecchio, R. Biasi, M. Andrighettoni, D. Gallieni, F. Zocchi, M. Lloyd-Hart, F. Wildi, H. M. Martin "The adaptive secondary mirror for the 6.5 conversion of the MMT, Beyond conventional adaptive optics", Venezia 2001, eds. R. Raggazzoni et S Esposito.
8. Low-cost, broadband static phase plate for generating atmospheric-like turbulence (Troy A. Rhoadarmer and J. Roger P. Angel) Applied Optics, 40, #18, 2946-2955, June 20, 2001.
9. Adaptive Optics at the 6.5 m MMT. (M. Lloyd-Hart, F. Wildi, H. Martin, P. McGuire, M. Kenworthy, R. Johnson, B. Fitz-Patrick, G. Angeli, S. Miller, R. Angel) SPIE Conference on Adaptive Optics Systems and Technology, ed. P. Wizinowich, 4007, 167-174, Munich, 2000.
10. Adaptive Secondary Mirror for the 6.5 m Conversion of the Multiple Mirror Telescope: Delivery Test Results (A. Riccardi, G. Brusa, V. Bilotti, C. Del Vecchio, P. Salinari, P. Stefanini, P. Mantegazza, R. Biasi, M. Andrighettoni, C. Franchini, D. Gallieni, M. Lloyd-Hart, P. McGuire, S. Miller, and H. Martin) *ibid.*, 524-531.
11. P.C. McGuire, M. Lloyd-Hart, J.R.P. Angel, G.Z. Angeli, R.L. Johnson, B.C. Fitzpatrick, W.B. Davison, R.J. Sarlot, C.J. Bresloff, J.M. Hughes, S.M. Miller, P. Schaller, F.P. Wildi, M.A. Kenworthy, R.M. Cordova, M.L.Rademacher, M.H. Rascon, J.H. Burge, B.L. Stamper, C.Zhao, P. Salinari, C.Del Vecchio, A. Riccardi, G.Brusa, R. Biasi, M. Andrighettoni, D. Gallieni, C. Franchini, D.G. Sandler, T.K. Barrett." Full-System Laboratory Testing of the F/15 Deformable Secondary Mirror for the New MMT Adaptive Optics System", SPIE Conference on Adaptive Optics Systems and Technology, ed s. R.Q. Fugate and R. K. Tyson, 3762, 28-37, Denver, 1999.
12. Hoffmann, W. F., Hora, J.L., Fazio, G.G., Deutsch, L.K., & Dayal, A. 1998 Proc. SPIE, 3354, 647.
13. M. Demerlé in Adaptive Optics for astronomy, proceedings of the NATO Advanced Study Institute, Kluwer Academic Publishers, 1994
14. Hinz, P.M., Angel, J.R.P., Woolf, N.W., Hoffmann, W.F., & McCarthy, D.W. 2000 Proc. SPIE 4006, 349